BRITISH JOURNAL OF HOSPITAL MEDICINE

ARTICLE

Prediction of Cervical Cancer Lymph Node Metastasis via a Multimodal Transfer Learning Approach

Yeqin Zhu[1], Chunlong Fu[2], Junqiang Du[1], Yuhui Jin[3], Shunlan Du[1,*], Fenhua Zhao[2,*]

[1]Department of Gynecology and Obstetrics, Affiliated Dongyang Hospital of Wenzhou Medical University, Dongyang, Zhejiang, China
[2]Department of Radiology, Affiliated Dongyang Hospital of Wenzhou Medical University, Dongyang, Zhejiang, China
[3]Department of Pathology, Affiliated Dongyang Hospital of Wenzhou Medical University, Dongyang, Zhejiang, China
*Correspondence: 13758953638@wmu.edu.cn (Shunlan Du); zhfenhua@163.com (Fenhua Zhao)

Abstract

Aims/Background In the treatment of patients with cervical cancer, lymph node metastasis (LNM) is an important indicator for stratified treatment and prognosis of cervical cancer. This study aimed to develop and validate a multimodal model based on contrast-enhanced multiphase computed tomography (CT) images and clinical variables to accurately predict LNM in patients with cervical cancer.

Methods This study included 233 multiphase contrast-enhanced CT images of patients with pathologically confirmed cervical malignancies treated at the Affiliated Dongyang Hospital of Wenzhou Medical University. A three-dimensional MedicalNet pre-trained model was used to extract features. Minimum redundancy-maximum correlation, and least absolute shrinkage and selection operator regression were used to screen the features that were ultimately combined with clinical candidate predictors to build the prediction model. The area under the curve (AUC) was used to assess the predictive efficacy of the model.

Results The results indicate that the deep transfer learning model exhibited high diagnostic performance within the internal validation set, with an AUC of 0.82, accuracy of 0.88, sensitivity of 0.83, and specificity of 0.89.

Conclusion We constructed a comprehensive, multiparameter model based on the concept of deep transfer learning, by pre-training the model with contrast-enhanced multiphase CT images and an array of clinical variables, for predicting LNM in patients with cervical cancer, which could aid the clinical stratification of these patients via a noninvasive manner.

Key words: cervical malignancy; lymph node metastasis; radiomics; deep learning; transfer learning

Submitted: 12 July 2024 Revised: 28 August 2024 Accepted: 3 September 2024

Introduction

Cervical cancer is a prevalent malignancy and the second leading cause of cancer-related mortality in women aged 20–39 (Siegel et al, 2023). Patients with early-stage cervical cancer without lymph node metastasis (LNM) have a high 5-year survival rate of up to 90%, whereas those with cervical cancer and LNM have a 5-year survival rate of only 65% (Bizzarri et al, 2021; Qin et al, 2024). The most recent staging system, developed by the International Federation of Gynecology and Obstetrics (FIGO), incorporates LNM into its staging schema, providing a pivotal criterion for tailored therapeutic interventions for cervical cancer (Maeda et al, 2024; Singh et al, 2023).

How to cite this article:
Zhu Y, Fu C, Du J, Jin Y, Du S, Zhao F. Prediction of Cervical Cancer Lymph Node Metastasis via a Multimodal Transfer Learning Approach. Br J Hosp Med. 2024. https://doi.org/10.12968/hmed.2024.0428

Radical hysterectomy and pelvic lymph node dissection (PLND) are recommended in the FIGO guidelines as standard treatments for stage IB–IIA cervical cancer. However, LNM arises in only 10–30% of patients with early-stage cervical cancer, meaning that a large proportion of these patients do not benefit from PLND while being at risk of associated adverse reactions and complications (Liu et al, 2023; Maeda et al, 2024). Fertility preservation surgery emerges as a favorable option for patients with cervical cancer who have not given birth or have childbearing needs, but this method is not suitable for patients with LNM. Therefore, accurate preoperative identification of LNM plays a crucial role in informing the treatment strategies for patients with cervical cancer (Manganaro et al, 2021). Currently, the diagnosis of LNM relies on lymphadenectomy and sentinel lymph node biopsy, which are invasive and retrospective procedures. This calls for a noninvasive method that can accurately assess LNM before surgery, providing a reliable reference for the clinical diagnosis and treatment of cervical cancer.

Imaging examination is an important strategy for the preoperative staging of cervical cancer, which can assess the extent of local invasion, LNM, and distant organ metastasis of the tumor to assist clinical decision-making for treatment and evaluate its efficacy. Every imaging modality has its own advantages and disadvantages. Pelvic magnetic resonance imaging (MRI) is the best imaging method for the local staging of cervical cancer with high soft tissue resolution, which is advantageous for evaluating the relationship of cervical lesions and surrounding structures (such as the bladder and rectum) with LNM (Manganaro et al, 2021). Positron emission tomography (PET)-computed tomography (CT) examination is considered the most effective method of evaluating LNM and is widely adopted as a standard procedure across numerous medical centers; however, this technique entails costly expenses, requires high-level technical expertise for operation, and involves high exposure to radiation (Chen et al, 2020; Manganaro et al, 2021). Compared with other imaging tests, CT imaging alone is the most widely used and popular technique in clinical practice, by virtue of its low operating costs and ability to scan a wide range of organs in the abdominopelvic cavity for detecting distant metastases. It is crucial to note that the accuracy of imaging assessment of LNM is limited primarily because it is judged by radiologists based on lymph node size and margins, additionally posing a subjective interpretation. Therefore, routine imaging assessments cannot avoid lymph node dissection or sampling in high-risk patients.

Radiomics can employ machine learning-based predictive models to automatically and thoroughly extract a large number of quantitative features from multimodal medical images and generate image markers. This approach is not influenced by the level of professional knowledge, subjective analysis, or the inherent limitations of traditional image interpretation. It is expected to improve the accuracy of the preoperative diagnosis of LNM in patients with cervical cancer. A previous study by Chen et al (2020) utilized CT images to establish radiomics models for predicting LNM in cervical cancer. However, the above study was limited by a relatively small sample size and the exclusion of clinical risk factors. Deep learning algorithms can automatically assign appropriate weights to each variable based on

their contributions, integrating this information to better identify the presence or absence of LNM. Various data modalities contain distinct categorical information.

Therefore, this study aimed to develop and validate a multimodal model based on contrast-enhanced multiphase CT images and clinical variables to accurately predict LNM in patients with cervical cancer. To this end, our study incorporated a larger study cohort, combining contrast-enhanced multiphase CT images and clinical variables, and constructed a model to predict LNM in patients with cervical cancer using a deep transfer learning approach.

Methods

Patients

This study was by approved the Affiliated Dongyang Hospital of Wenzhou Medical University review board and owing to the retrospective nature of the current investigation, the need for informed consent was waived by the Domain Specific Review Board. The study was performed in accordance with the principles set forth in the Declaration of Helsinki. In this study, patients with pathologically confirmed cervical cancer treated at the Affiliated Dongyang Hospital of Wenzhou Medical University from 1 January 2013 to 31 December 2023 were enrolled.

The patients were included based on the following criteria: (a) patients with pathologically confirmed cervical cell carcinoma; (b) patients who had received radical hysterectomy and PLND; (c) patients who did not receive preoperative treatment; and (d) patients who had undergone a standard CT examination within 1 month prior to surgery.

The exclusion criteria of this study are as follows: (a) patients who had received preoperative neoadjuvant radiotherapy; (b) patients with incomplete CT images; (c) patients with poor-quality CT images due to motion; and (d) patients with lesions that were too small to be visualized on CT. Fig. 1 shows the flowchart of patient recruitment for the present study.

Finally, 233 patients with cervical cancer who met the criteria were randomly assigned to a training set (n = 187), a test set (n = 23), and an independent validation set (n = 23), in a ratio of 8:1:1. Basic information, laboratory tests, and clinical characteristics were extracted from electronic medical records, whereas histological grades, pathological tumor-node-metastasis stages, and LNM information were obtained from pathology reports.

Image Acquisition

All CT scans in our center were performed with the patient lying in the supine position with the head advanced, and the range included all areas from the top of the liver septum to the bottom of the pelvis. The CT image acquisition was performed using scanners of the following models: Canon Aquilion ONE, Philips Brilliance, Siemens Force, and Siemens Definition. The scanning parameters of each CT scanner model are shown in Table 1.

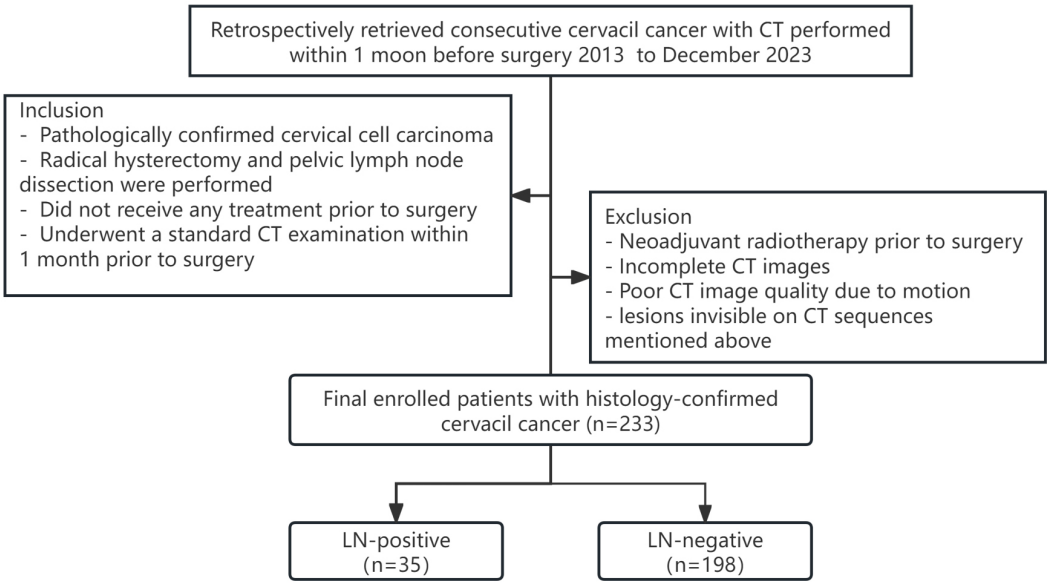

Fig. 1. Flowchart of patient recruitment in this study. Abbreviation: LN, lymph node; CT, computed tomography.

Table 1. Acquisition parameters for CT protocols.

Machine type	Philips Brilliance	Siemens Force	Siemens Definition	Canon Aquilion ONE
Row	64	96	62	16
Tube voltage (kV)	120	120	120	120
Effective power of tube (MA)	150	Auto	Auto	Auto
Matrix	1024 × 1024	512 × 512	512 × 512	512 × 512
Slice thickness (mm)	5	5	5	5

Model Development Framework

A major limitation in predicting cervical cancer LNM is the scarcity of available data, which imposes constraints on the model-training process. To address this issue, we selected MedicalNet by Chen et al (2019) as the pre-trained model and fine-tuned it for the downstream prediction task. MedicalNet is built upon ResNet by Hou et al (2020), which are widely used neural networks across various real-world applications, and pre-trained on a large-scale medical dataset across diverse modalities. The pre-trained model provides a strong starting point that enables the models to capture detailed representations in the dataset.

To enhance the recognition capability of our models, we used multimodal datasets comprising clinical data and CT images collected from each patient. Clinical data were categorized into two types: (i) Categorical data were presented as integer values corresponding to various categories, such as basic diseases, where 0, 1, and 2 denoted hypertension, diabetes, and other diseases, respectively. We employed a series of embedding layers to encode categorical data in a latent space. The primary design rationale for employing embedding layers was to augment the representational capacity of each data value, thereby providing ample capacity for neural networks to capture pertinent features related to prediction classes. (ii) Continuous

data, such as carcinoembryonic antigen (CEA) values and N transfer numbers, were normalized to a range of 0–1 to mitigate training instability.

The rationale for choosing embedding layers and a normalization process for continuous data comprises two main parts: The first part was to enhance model capacity. Some clinical data are discrete, such as nerve involvement data, which can only be 0 or 1 and may not be sufficiently informative for neural network learning. Embedding layers can transform discrete data into high-dimensional features, increasing the model's capacity to capture complex relationships within the data. The second part was to ensure numerical stability. Neural network training can sometimes be unstable due to large numbers causing the final output to exceed the numerical limit, resulting in 'nan' values. Additionally, data ranges can vary significantly, with some data ranging from 1 to 10 and others from 0 to 0.01. Without normalization, the latter data might be ignored during training. Therefore, to enhance training stability and model capacity, we introduced embedding layers and a normalization process. Intuitively, we aimed to balance the clinical data's importance with that of the CT images, so we chose an embedding dimension of 512, the same as the feature embeddings from the pre-trained MedicalNet. However, we empirically found that a dimension of 256 also worked well in this case.

The overarching framework of the proposed methodology is shown in Fig. 2. We used MedicalNet as the backbone to extract features from CT images, mapping the raw CT images into 512-dimension feature embeddings. The parameters for MedicalNet are inherited from the pre-trained model, which had been trained on large-scale medical data. Other parts of our framework, including the embedding layer and final multilayer perceptron (MLP) blocks (as shown in Fig. 2), are initialized with random values. In our experiments, we used an embedding layer to transform the original clinical data into high-dimensional embeddings, specifically using 512 dimensions to ensure that the model had sufficient capacity to capture the clinical data information. We empirically verified that 512 dimensions worked well. Next, we conducted a learning rate sweep from $1e^{-5}$ to $1e^{-1}$ and found that $1e^{-3}$ yielded the best performance. Fine-tuning the model from pre-trained weights requires careful selection of the learning rate; a high learning rate (e.g., $1e^{-1}$) can cause feature collapse from the pre-trained knowledge, leading to poor performance, while a low learning rate (e.g., $1e^{-5}$) is insufficient for learning from the downstream data. Subsequently, we set a weight decay of $1e^{-4}$ in the stochastic gradient descent (SGD) optimizer to alleviate overfitting, as the number of training data is limited due to practical constraints. Finally, all extracted features were concatenated and passed through an MLP block to generate predictions.

Model Development Implementation

Before training, we performed data augmentation on the raw CT images through random cropping. Firstly, we used the 'RandomResizedCrop' function from the PyTorch package. For each raw image, a random sub-image was cropped, with the crop area ranging from 0.08 to 1.0 of the original image. The size of the cropped image varies between 0.75 and 1.33 times the size of the crop area. This sub-image was then resized to 224 $\times$ 224 using bilinear interpolation. The position and size

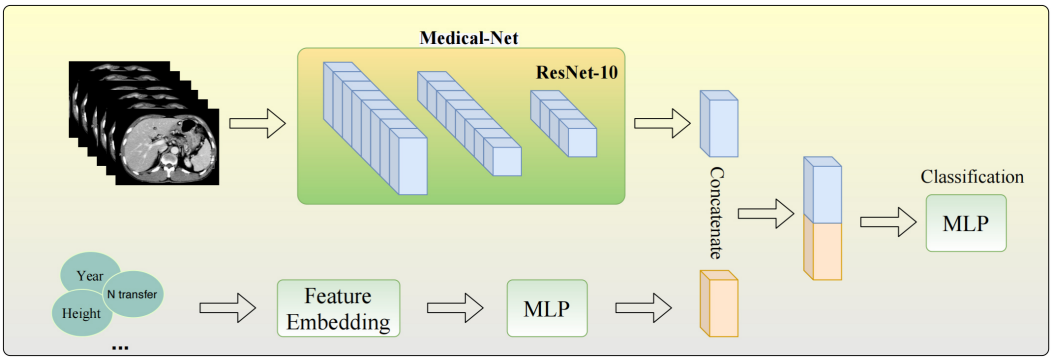

Fig. 2. Schematic depicting the framework of model development. The figure is drawn with the open-source python package matplotlib of version: 3.4.1 (https://matplotlib.org/stable/users/index.html.). Abbreviation: MLP, multilayer perceptron.

of the crop area follow the default hyperparameters, which generally provide better performance. Additionally, we incorporated random horizontal flipping with a 0.5 probability to further augment the data.

To address the severe class imbalance present in the dataset, we implemented a weighted sampling strategy, in which classes with fewer samples had a higher probability of being selected, with the probability being inversely proportional to the sample size. This ensured that each class had a similar probability of appearance during the training process. We randomly allocated 80% of the samples to the training set and 10% each to the validation and test sets. During training, we used the SGD optimizer with a momentum of 0.99 and a weight decay of $1e^{-4}$ to prevent overfitting. The initial learning rate was set at $1e^{-3}$ and adjusted using a cosine annealing schedule. The model underwent a warm-up phase of two epochs and was trained for 10 epochs. All models were implemented in PyTorch, and an NVIDIA RTX A6000 GPU was utilized for computation.

Validation and Evaluation of Models

The potential sources of bias in our study might stem from variations among patients, as individuals living in different areas may exhibit different characteristics, leading to bias. To mitigate this potential bias during the internal validation process, we randomly assigned 10% of the data to the validation set and used it to select the best model checkpoint. We also randomly allocated another 10% of the data into the test set and reported our results based on this test set. To further examine potential bias, we plan to collect data from other hospitals to evaluate the generalizability of our model in future study.

To quantitatively assess the performance of our model in recognizing cervical cancer LNM, we utilized several metrics, including accuracy (ACC = TP + TN/TP + TN + FP + FN), sensitivity (SE = TP/TP + FN), specificity (SP = TN/TN + FP), and area under the curve (AUC) of the receiver operating characteristic (ROC), where TN, TP, FP, and FN represent true negative, true positive, false positive, and false negative, respectively.

Table 2. Clinicopathological characteristics of patients.

Characteristics	Total n percentile (n = 233)		*p*	Value
	LN+ (n = 35)	LN– (n = 198)		
Age (mean ± SD, years)	53.43 ± 9.68	53.82 ± 10.33	0.834	$t = 0.210$
CEA level			0.012*	$\chi^2 = 6.378$
Normal (<5 ng/mL)	24 (68.6%)	170 (85.9%)		
Elevated (≥5 ng/mL)	11 (31.4%)	28 (14.1%)		
CA 19-9 level			0.007*	$\chi^2 = 7.356$
Normal (<37 U/mL)	30 (85.7%)	193 (97.5%)		
Elevated (≥37 U/mL)	5 (14.3%)	5 (2.5%)		
CA 125 level			0.000*	$\chi^2 = 12.941$
Normal (<35 U/mL)	29 (82.9%)	187 (94.4%)		
Elevated (≥35 U/mL)	6 (17.1%)	11 (5.6%)		
SCC-Ag level			0.006*	$\chi^2 = 7.636$
Normal (<1.5 ng/mL)	9 (25.7%)	101 (51.0%)		
Elevated (≥1.5 ng/mL)	26 (74.3%)	97 (49.0%)		
Clinical stage			0.000*	$\chi^2 = 180.866$
FIGO I–II	4 (11.4%)	193 (97.5%)		
FIGO III–IV	31 (88.6%)	5 (2.5%)		
Differentiation Grade			0.403	$\chi^2 = 0.699$
Well/Moderately differentiated	27 (77.1%)	139 (70.2%)		
Poorly/undifferentiated	8 (22.9%)	59 (29.8%)		
Pathological LVI status			0.000*	$\chi^2 = 13.104$
Positive	19 (54.3%)	48 (24.2%)		
Negative	16 (45.7%)	150 (75.8%)		
Pathological PNI status			0.746	$\chi^2 = 0.105$
Positive	4 (11.4%)	16 (8.1%)		
Negative	31 (88.6%)	182 (91.9%)		

Continuous variables like age are expressed as means ± standard deviation. For categorical variables such as CEA, SCC-Ag, FIGO, LVI and Differentiation Grade, the expected values are all greater than 5, and thus, Chi-square test was used. For categorical variables such as CA19-9, CA125 and PNI, at least one expected value is less than 5, but greater than 1, and thus, Calibrated chi-square test was employed. Unless otherwise indicated, data are expressed as count, denoting the number of patients, with percentages in parentheses. *, $p < 0.05$. Abbreviations: SD, standard deviation; CEA, carcinoembryonic antigen; CA19-9, carbohydrate antigen 19-9; CA125, carbohydrate antigen 125; SCC-Ag, squamous cell carcinoma antigen; FIGO, International Federation of Gynecology and Obstetrics; LN–, lymph node-negative; LN+, lymph node-positive; LVI, lymphovascular invasion; PNI, perineural invasion; Differentiation Grade, pathological tumor histological grade.

Statistical Analysis

Statistical Package for the Social Sciences (SPSS) software (version 26.0, IBM Corp., Armonk, NY, USA) was used to perform statistical analyses of the queue data. The Shapiro–Wilk test was employed to analyze whether the quantitative data followed a normal distribution. Normally distributed data are expressed as mean ±

standard deviation, whereas data that did not follow a normal distribution are presented as median (Q1, Q3). For comparison between the two groups, independent sample *t*-tests or Mann–Whitney *U* tests were utilized. Data of categorical variables are presented as frequencies and percentages. Such data were analyzed using the Chi-square tests test when the expected values were greater than or equal to 5, at least one expected value is less than 5, but greater than 1, and thus, Calibrated chi-square test was employed. Statistical significance was set at $p < 0.05$.

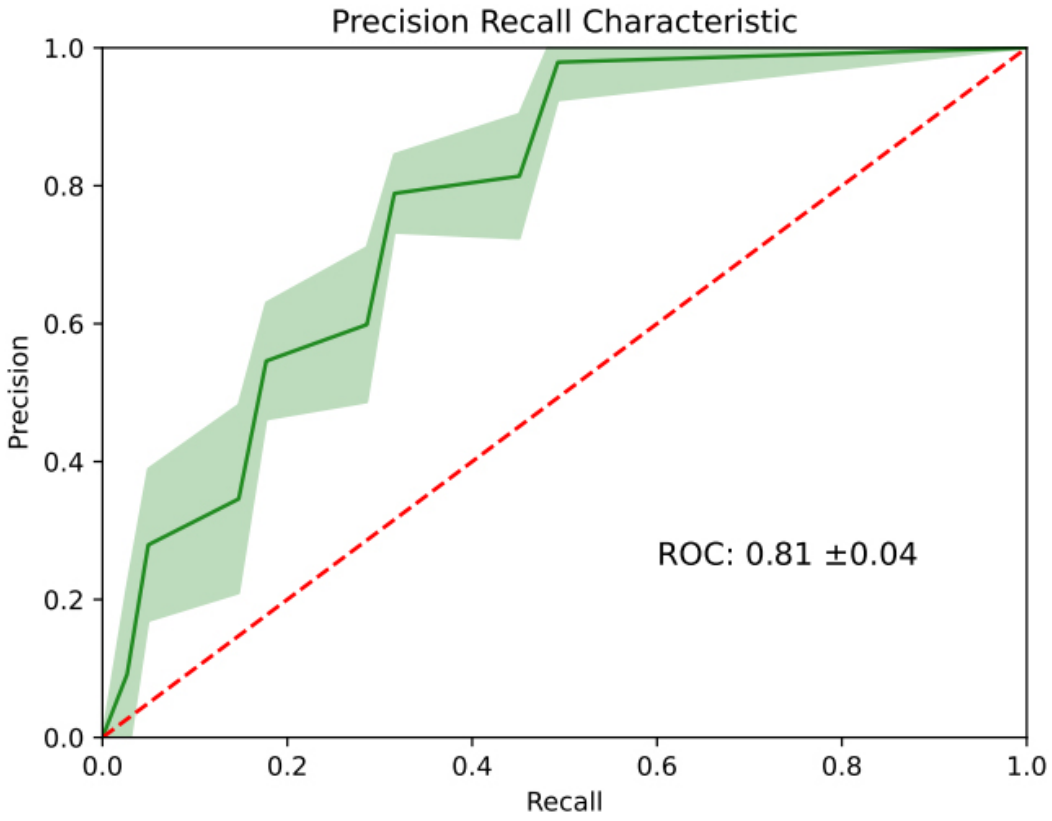

Fig. 3. ROC curve of the combined model of CT image and clinical factors. Abbreviations: ROC, receiver operating characteristic.

Results

Patient Characteristics

The 233 patients eligible for inclusion were categorized into lymph node-positive (LN+) group (n = 35) and lymph node-negative (LN–) group (n = 198) according to the surgical pathology results. The mean ages of the LN+ and LN– groups were 53.43 ± 9.68 and 53.82 ± 10.33 years, respectively, with no significant difference in the mean ages between the groups. In addition, there was no significant difference in differentiation grade and pathological perineural invasion (PNI) status between the two groups, but significant differences were detected between the two groups in terms of carcinoembryonic antigen (CEA) level, carbohydrate antigen (CA) 19-9 level, CA 125 level, squamous cell carcinoma antigen (SCC-Ag) level,

Table 3. Results of lymph node classification.

Methods	ACC (%)	SE (%)	SP (%)	ROC (%)	PPV (%)	NPV (%)
W. CT image	0.71 ± 0.03	0.58 ± 0.07	0.79 ± 0.01	0.60 ± 0.02	0.67 ± 0.01	0.83 ± 0.02
W. Clinical data	0.77 ± 0.04	0.67 ± 0.08	0.70 ± 0.09	0.70 ± 0.09	0.62 ± 0.11	0.86 ± 0.02
W. Multi-Modal	0.87 ± 0.05	0.82 ± 0.10	0.89 ± 0.04	0.81 ± 0.04	0.77 ± 0.08	0.94 ± 0.02

Abbreviations: ACC, accuracy; ROC, receiver operating characteristic; CT, computed tomography, NPV, negative predictive value; PPV, positive predictive value; SE, sensitivity; SP, specificity.

clinical stage, and pathological lymphovascular invasion (LVI) status. Detailed statistical data on the baseline characteristics are shown in Table 2.

Predictive Performance of the Model

First, we present the end-to-end results of our approach in Table 3. Our model, which employs multimodal data, achieved a test accuracy of 87% for lymph node classification, demonstrating its superior effectiveness. Additionally, we visualized the corresponding ROC curves in Fig. 3, which demonstrate encouraging results. Notably, our framework achieves a large AUC of 0.81 ± 0.04, compared to the single-modal data results with AUC of 0.62 ± 0.02 and 0.70 ± 0.09, which are significantly smaller and exhibit no overlap in the error bars with our multi-modal method. Given the significant class imbalance in the test data, there is a potential risk that the model will consistently predict a single class. Further analyses showed that the model possesses the ability to recognize any class with high-level sensitivity and specificity.

Furthermore, we conducted an ablation study to investigate the individual contributions of CT images and clinical data to model performance. As shown in Table 3, although single-modal data can achieve relatively high accuracy (over 70%) in classification tasks, they consistently and significantly underperform compared with our multimodal data-driven predictive approach. Intuitively, by incorporating more relevant data, the model can capture more meaningful features associated with the output, resulting in superior performance.

Discussion

This study developed and validated an integrated model combining contrast-enhanced multiphase CT images and clinical variables that can be used to accurately predict LNM in patients with cervical cancer and may assist in the clinical development of personalized treatment plans.

LNM is a significant risk factor affecting patient prognosis and an important criterion for the stratified treatment of cervical cancer (Maeda et al, 2024; Singh et al, 2023). Preoperative assessment is crucial in patients with cervical cancer. At present, imaging remains the primary clinical method for assessing LNM, with ultrasound being inadequate for evaluating the deep pelvic and para-aortic lymph nodes in patients with cervical cancer. CT and MRI have advantages in displaying tumors and adjacent structures, and their assessment of LNM mainly depends on the

physician's experience in interpreting features such as LNM, morphology, signal, and enhancement characteristics. PET/CT can enhance the detection rate of LNM; however, a previous study has reported that CT, MRI, and PET have high specificity but low sensitivity in LNM detection (Woo et al, 2020). Thus, these methods have limitations in assessing LNM in pelvic malignancies (Fruhauf et al, 2024; Rockall et al, 2021; Woo et al, 2020). Radiomic approaches have been utilized in several studies to assess LNM in cervical cancer. Chen et al (2020) constructed a model based on CT images to predict LNM in patients with cervical cancer. Although their study demonstrated the feasibility of the preoperative CT radiomics features in predicting LNM in cervical cancer, the sample size used was relatively small and the segmentation of region of interest (ROI) was implemented via a manual approach, which required a tremendous amount of work. The rise of artificial intelligence has provided various possibilities for medical and clinical advancements. This technology possesses the capability of high-throughput data mining and provides a large amount of additional information for clinical applications (Shur et al, 2021). Our study differs from previous studies in that we harnessed deep-learning methods to automatically delineate the ROIs and used transfer learning to construct a predictive model. The combination of automatic segmentation and deep transfer learning can improve work efficiency and enhance the robustness of the model. In our study, the constructed deep learning model demonstrated moderate predictive performance in forecasting LNM in cervical cancer, with an AUC of 0.62, accuracy of 0.71, sensitivity of 0.58, and specificity of 0.79.

In this study, we select potential clinical candidate predictors from previous literature. However, in the univariate regression analysis, only preoperative SCC-Ag, clinical stage, and pathological LVI status showed a significant difference between the groups with and without LNM. In response to this situation, the prevalent strategy is to exclude variables that do not show statistical significance from the final model. Nevertheless, according to the previous study, statistical non-significance does not necessarily imply clinical irrelevance (Dong et al, 2020). Additionally, deep learning methods are, to some extent, black boxes that can automatically assign appropriate weights to each variable based on their contributions. Therefore, we included clinical candidate predictors that showed no statistical significance in the construction of our predictive model. Our results indicate that the model built by incorporating all potential clinical candidate predictors performs well in predicting LNM in patients with cervical cancer, with an AUC of 0.70, an accuracy of 0.77, a sensitivity of 0.64, and a specificity of 0.81.

Different data modalities contain different categorical information, and deep learning can extract and integrate this information to better identify the presence or absence of LNM. Hou et al (2020) constructed a multimodal model by extracting radiomics information from T2-weighted image, apparent diffusion coefficient, and enhanced T1-weighted image, and combining it with clinical variables to predict LNM in patients with cervical cancer, demonstrating that the multi-parameter model outperformed the single-parameter model. Their study inspired us to construct a comprehensive model, based on deep learning features extracted from contrast-enhanced multiphase CT images and clinical candidate predictors, to predict LNM

in cervical cancer. This comprehensive model showed superior prediction performance, with an AUC as high as 0.81, and accuracy, sensitivity, and specificity rates all exceeding 80%.

Additionally, our model holds promising clinical application potential. It is important to note that most cervical cancer patients would not benefit from the standard treatment (i.e., PLND) due to delayed diagnosis and fertility preservation surgery is not suitable for patients with LNM. Given these critical challenges, the accurate preoperative identification of LNM stands as a crucial avenue for preserving fertility among early-stage cervical cancer patients with childbearing desires, representing an urgent clinical need. Our study has developed an integrated model that combines contrast-enhanced multiphase CT imaging and clinical variables, which can accurately predict LNM in cervical cancer patients preoperatively. This model can assist clinicians in more accurately determining the presence of LNM in early-stage cervical cancer patients, thereby effectively augmenting fertility preservation in patients with childbearing needs. Moreover, the most common sites for LNM in cervical cancer are the external iliac, internal iliac, and obturator regions, whereas the less common sites, such as the common iliac, presacral, and abdominal aortic areas, are not typically included in standard pelvic lymph node dissection surgery. Another value added to the comprehensive model constructed in this study is its higher accuracy in the identification of LNM in these less common regions, aiding in the preoperative planning of surgical approaches.

This study has some limitations. Firstly, this was a retrospective study, which has potential bias and should be replicated in a prospective study to validate the constructed model. Secondly, this is a single-center study, potentially yielding data that are not sufficiently representative; therefore, a larger, multicenter external cohort is needed to test the predictive performance and robustness of the constructed model. In further research, we shall perform external validation of our model using partial data collected from two other centers, as well as conduct prospective validation of the model using cases in our center. Thirdly, the current model was not validated in different populations and using different imaging techniques; this necessitates model validation in different demographic groups and using different imaging protocols in further studies.

Conclusion

In summary, we constructed a comprehensive, multiparameter model based on the concept of deep transfer learning, by pre-training the model with contrast-enhanced multiphase CT images and an array of clinical variables, for predicting LNM in patients with cervical cancer, which could aid the clinical stratification of these patients via a noninvasive manner.

Key Points

- Lymph node metastasis is a significant risk factor affecting patient prognosis and an important criterion for the stratified treatment of cervical cancer.
- The primary design rationale for employing embedding layers was to augment the representational capacity of each data value, thereby providing ample capacity for neural networks to capture pertinent features related to prediction classes.
- By incorporating more relevant data, the model can capture more meaningful features associated with the output, resulting in a superior performance.
- The model has a high classification accuracy, sensitivity, and specificity of 87%, 82%, and 89%, respectively, demonstrating the potential to facilitate early diagnosis of cervical cancer.

Availability of Data and Materials

The datasets generated and/or analysed during the current study are not publicly available due to restrictions of the Affiliated Dongyang Hospital of Wenzhou Medical University review board to protect patient's privacy but are available from the corresponding authors on reasonable request.

Author Contributions

YQZ and CLF: Conceptualisation, methodology, writing—original draft; JQD: Data curation, formal analysis; YHJ: Investigation, data curation, methodology; FHZ and SLD: Conceptualisation, supervision, writing—review and editing. All authors contributed to important editorial changes in the manuscript. All authors have read and approved the final version of the manuscript. All authors have participated sufficiently in the work and agreed to be accountable for all aspects of the work.

Ethics Approval and Consent to Participate

This study was conducted in compliance with ethical standards and has been approved by the Affiliated Dongyang Hospital of Wenzhou Medical University review board (approval number: 2024-YX-125). The need for informed consent was waived by the Domain Specific Review Board. The study was performed in accordance with the principles set forth in the Declaration of Helsinki.

Acknowledgement

Not applicable.

Funding

This research was supported by the Zhejiang Medicine and Health Science and Technology Project (grant no. 2023ZL751).

Conflict of Interest

The authors declare no conflict of interest.

References

Bizzarri N, Boldrini L, Ferrandina G, Fanfani F, Pedone Anchora L, Scambia G, et al. Radiomic models for lymph node metastasis prediction in cervical cancer: can we think beyond sentinel lymph node? Translational Oncology. 2021; 14: 101185. https://doi.org/10.1016/j.tranon.2021.101185

Chen S, Ma K, Zheng Y. Med3d: Transfer learning for 3d medical image analysis. arXiv. 2019. https://doi.org/10.48550/arXiv.1904.00625

Chen X, Liu W, Thai TC, Castellano T, Gunderson CC, Moore K, et al. Developing a new radiomics-based CT image marker to detect lymph node metastasis among cervical cancer patients. Computer Methods and Programs in Biomedicine. 2020; 197: 105759. https://doi.org/10.1016/j.cmpb.2020.105759

Dong T, Yang C, Cui B, Zhang T, Sun X, Song K, et al. Development and Validation of a Deep Learning Radiomics Model Predicting Lymph Node Status in Operable Cervical Cancer. Frontiers in Oncology. 2020; 10: 464. https://doi.org/10.3389/fonc.2020.00464

Fruhauf F, Cibula D, Kocian R, Zikan M, Dundr P, Jarkovsky J, et al. Diagnostic performance of ultrasonography in pre-operative assessment of lymph nodes in patients with cervical cancer. International Journal of Gynecological Cancer. 2024; 34: 985–992. https://doi.org/10.1136/ijgc-2024-005341

Hou L, Zhou W, Ren J, Du X, Xin L, Zhao X, et al. Radiomics Analysis of Multiparametric MRI for the Preoperative Prediction of Lymph Node Metastasis in Cervical Cancer. Frontiers in Oncology. 2020; 10: 1393. https://doi.org/10.3389/fonc.2020.01393

Liu S, Zhou Y, Wang C, Shen J, Zheng Y. Prediction of lymph node status in patients with early-stage cervical cancer based on radiomic features of magnetic resonance imaging (MRI) images. BMC Medical Imaging. 2023; 23: 101. https://doi.org/10.1186/s12880-023-01059-6

Maeda M, Mabuchi S, Sakata M, Deguchi S, Kakubari R, Matsuzaki S, et al. Significance of tumor size and number of positive nodes in patients with FIGO 2018 stage IIIC1 cervical cancer. Japanese Journal of Clinical Oncology. 2024; 54: 146–152. https://doi.org/10.1093/jjco/hyad141

Manganaro L, Lakhman Y, Bharwani N, Gui B, Gigli S, Vinci V, et al. Staging, recurrence and follow-up of uterine cervical cancer using MRI: Updated Guidelines of the European Society of Urogenital Radiology after revised FIGO staging 2018. European Radiology. 2021; 31: 7802–7816. https://doi.org/10.1007/s00330-020-07632-9

Qin F, Sun X, Tian M, Jin S, Yu J, Song J, et al. Prediction of lymph node metastasis in operable cervical cancer using clinical parameters and deep learning with MRI data: a multicentre study. Insights into Imaging. 2024; 15: 56. https://doi.org/10.1186/s13244-024-01618-7

Rockall AG, Barwick TD, Wilson W, Singh N, Bharwani N, Sohaib A, et al. Diagnostic Accuracy of FEC-PET/CT, FDG-PET/CT, and Diffusion-Weighted MRI in Detection of Nodal Metastases in Surgically Treated Endometrial and Cervical Carcinoma. Clinical Cancer Research. 2021; 27: 6457–6466. https://doi.org/10.1158/1078-0432.CCR-21-1834

Shur JD, Doran SJ, Kumar S, Ap Dafydd D, Downey K, O'Connor JPB, et al. Radiomics in Oncology: A Practical Guide. Radiographics. 2021; 41: 1717–1732. https://doi.org/10.1148/rg.2021210037

Siegel RL, Miller KD, Wagle NS, Jemal A. Cancer statistics, 2023. CA: A Cancer Journal for Clinicians. 2023; 73: 17–48. https://doi.org/10.3322/caac.21763

Singh D, Vignat J, Lorenzoni V, Eslahi M, Ginsburg O, Lauby-Secretan B, et al. Global estimates of incidence and mortality of cervical cancer in 2020: a baseline analysis of the WHO Global Cervical Cancer

Elimination Initiative. The Lancet. Global Health. 2023; 11: e197–e206. https://doi.org/10.1016/S2214-109X(22)00501-0

Woo S, Atun R, Ward ZJ, Scott AM, Hricak H, Vargas HA. Diagnostic performance of conventional and advanced imaging modalities for assessing newly diagnosed cervical cancer: systematic review and meta-analysis. European Radiology. 2020; 30: 5560–5577. https://doi.org/10.1007/s00330-020-06909-3